Argon ICP Global Model

Technical Documentation

0D Plasma Chemistry Model for Gridded Ion Thruster
Alternative Propellants Study

Khoi Nguyen

January 2026

Based on: Magaldi et al., "A Global Model Study of Plasma Chemistry and Propulsion Parameters of a Gridded Ion Thruster Using Argon as Propellant," *Plasma* 2022, 5, 324–340.

Contents

1 Introduction

This document provides comprehensive technical documentation for a 0D global plasma model developed for an Argon Inductively Coupled Plasma (ICP) gridded ion thruster. The model was developed as part of ongoing studies on alternative propellants for electric propulsion systems.

1.1 Background and Motivation

Global (0D) plasma models provide a computationally efficient approach to studying plasma chemistry by solving volume-averaged particle and energy balance equations. While full 2D/3D simulations capture spatial variations, they are computationally expensive—often requiring hours per operating point. A validated 0D model enables rapid parameter sweeps suitable for design optimization and sensitivity analysis.

The reference for this work is Magaldi et al. (2022) [1], who developed a 0D global model for an argon ICP thruster implemented in COMSOL Multiphysics. Our implementation reproduces their model in MATLAB, with necessary modifications to handle terms that COMSOL computes internally (such as boundary conditions and gas flow) but must be explicitly coded in a standalone implementation.

1.2 Objectives

1. Implement the 0D global model equations from Magaldi et al. in MATLAB
2. Validate against the published COMSOL reference data
3. Achieve species density errors $< 5\%$ and gas temperature errors $< 1\%$
4. Generate training data for neural network surrogate model development
5. Document limitations and potential improvements for future work

1.3 Model Overview

The model tracks seven state variables:

$$\mathbf{y} = \begin{bmatrix} n_{\mathrm{Ar}} & n_{\mathrm{Ar}^m} & n_{\mathrm{Ar}^r} & n_{\mathrm{Ar}^p} & n_{\mathrm{I}} & T_e & T_g \end{bmatrix}^T \tag{1}$$

representing five argon species densities (ground state, metastable, resonant, 4p excited, and ions) plus electron and gas temperatures. The model assumes quasi-neutrality ($n_e = n_{\mathrm{I}}$) and solves coupled ODEs for particle and energy balance.

1.4 Operating Conditions

The model is configured for the following nominal conditions from the reference paper:

Table 1: Nominal Operating Parameters

Parameter	Value	Description
R	6 cm	Chamber radius
L	10 cm	Chamber length
p_0	2 mTorr (0.267 Pa)	Operating pressure
P_{RF}	225–1575 W	RF power range
f_{RF}	13.56 MHz	RF frequency
$T_{g,0}$	300 K	Wall temperature
V_{grid}	1000 V	Grid voltage
β_i	0.7	Ion grid transparency
β_g	0.3	Neutral grid transparency

2 Species Balance Equations: `rhs_global.m`

The main ODE function `rhs_global.m` defines the system of coupled differential equations for all seven state variables. This section presents the complete mathematical formulation.

2.1 Reaction Chemistry

The model implements 20 reactions organized into categories:

Table 2: Argon Reaction Set

Rate	Reaction	Type	Threshold
k_1	$e + \mathrm{Ar} \to e + \mathrm{Ar}$	Elastic	–
k_2	$e + \mathrm{Ar} \to \mathrm{Ar}^+ + 2e$	Direct ionization	15.76 eV
k_3	$e + \mathrm{Ar}^m \to \mathrm{Ar}^+ + 2e$	Stepwise ionization	4.43 eV
k_4	$e + \mathrm{Ar}^r \to \mathrm{Ar}^+ + 2e$	Stepwise ionization	3.96 eV
k_5	$e + \mathrm{Ar}^p \to \mathrm{Ar}^+ + 2e$	Stepwise ionization	2.26 eV
k_6	$e + \mathrm{Ar} \to e + \mathrm{Ar}^m$	Excitation	11.5 eV
k_7	$e + \mathrm{Ar} \to e + \mathrm{Ar}^r$	Excitation	11.6 eV
k_8	$e + \mathrm{Ar} \to e + \mathrm{Ar}^p$	Excitation	12.9 eV
k_9	$e + \mathrm{Ar}^m \to e + \mathrm{Ar}$	De-excitation	–
k_{10}	$e + \mathrm{Ar}^r \to e + \mathrm{Ar}$	De-excitation	–
k_{11}	$e + \mathrm{Ar}^p \to e + \mathrm{Ar}$	De-excitation	–
k_{12}	$e + \mathrm{Ar}^m \to e + \mathrm{Ar}^r$	Transfer	–
k_{13}	$e + \mathrm{Ar}^m \to e + \mathrm{Ar}^p$	Transfer	–
k_{14}	$e + \mathrm{Ar}^r \to e + \mathrm{Ar}^p$	Transfer	–
k_{15}	$e + \mathrm{Ar}^r \to e + \mathrm{Ar}^m$	Transfer	–
k_{16}	$e + \mathrm{Ar}^p \to e + \mathrm{Ar}^m$	Transfer	–
k_{17}	$e + \mathrm{Ar}^p \to e + \mathrm{Ar}^r$	Transfer	–
k_{18}	$\mathrm{Ar}^r \to \mathrm{Ar} + h\nu$	Radiative decay	–
k_{19}	$\mathrm{Ar}^p \to \mathrm{Ar}^m + h\nu$	Radiative decay	–
k_{20}	$\mathrm{Ar}^p \to \mathrm{Ar}^r + h\nu$	Radiative decay	–

2.2 Rate Coefficient Expressions

Rate coefficients are implemented in `RateCoefficients_Ar.m` as Arrhenius-type expressions. Units: k_1–k_{17} in $\mathrm{m^3\,s^{-1}}$; k_{18}–k_{20} in $\mathrm{s^{-1}}$.

Elastic collision:

$$k_1 = 2.3 \times 10^{-14}\, T_e^{1.61} \exp\left(0.06(\ln T_e)^2 - 0.12(\ln T_e)^3\right) \tag{2}$$

Ionization (direct and stepwise):

$$k_2 = 2.39 \times 10^{-14}\, T_e^{0.57} \exp(-17.43/T_e) \tag{3}$$
$$k_3 = 2.71 \times 10^{-13}\, T_e^{0.26} \exp(-4.59/T_e) \tag{4}$$
$$k_4 = 2.71 \times 10^{-13}\, T_e^{0.28} \exp(-4.24/T_e) \tag{5}$$
$$k_5 = 1.09 \times 10^{-12}\, T_e^{0.29} \exp(-3.42/T_e) \tag{6}$$

Excitation (ground to excited states):

$$k_6 = 2.5 \times 10^{-15}\, T_e^{0.74} \exp(-11.56/T_e) \qquad (\mathrm{Ar} \to \mathrm{Ar}^m) \tag{7}$$
$$k_7 = 3.93 \times 10^{-15}\, T_e^{0.46} \exp(-12.09/T_e) \qquad (\mathrm{Ar} \to \mathrm{Ar}^r) \tag{8}$$
$$k_8 = 8.91 \times 10^{-15}\, T_e^{-0.04} \exp(-14.18/T_e) \qquad (\mathrm{Ar} \to \mathrm{Ar}^p) \tag{9}$$

De-excitation (superelastic, excited to ground):

$$k_9 = 2.25 \times 10^{-16}\, T_e^{-0.17} \exp(-1.65/T_e) \qquad (\mathrm{Ar}^m \to \mathrm{Ar}) \tag{10}$$
$$k_{10} = 6.82 \times 10^{-16}\, T_e^{0.44} \exp(-0.43/T_e) \qquad (\mathrm{Ar}^r \to \mathrm{Ar}) \tag{11}$$
$$k_{11} = 2.97 \times 10^{-16}\, T_e^{-0.11} \exp(-1.38/T_e) \qquad (\mathrm{Ar}^p \to \mathrm{Ar}) \tag{12}$$

Excited state transfers:

$$k_{12} = 3.7 \times 10^{-13} \qquad (\mathrm{Ar}^m \to \mathrm{Ar}^r) \tag{13}$$
$$k_{13} = 2.39 \times 10^{-12}\, T_e^{-0.15} \exp(-1.82/T_e) \qquad (\mathrm{Ar}^m \to \mathrm{Ar}^p) \tag{14}$$
$$k_{14} = 2.48 \times 10^{-12}\, T_e^{-0.16} \exp(-1.79/T_e) \qquad (\mathrm{Ar}^r \to \mathrm{Ar}^p) \tag{15}$$
$$k_{15} = 9.1 \times 10^{-13} \qquad (\mathrm{Ar}^r \to \mathrm{Ar}^m) \tag{16}$$
$$k_{16} = 1.5 \times 10^{-13}\, T_e^{0.51} \qquad (\mathrm{Ar}^p \to \mathrm{Ar}^m) \tag{17}$$
$$k_{17} = 1.5 \times 10^{-13}\, T_e^{0.51} \qquad (\mathrm{Ar}^p \to \mathrm{Ar}^r) \tag{18}$$

Radiative decay (first-order, units of $\mathrm{s^{-1}}$):

$$k_{18} = 1.0 \times 10^{5} \qquad (\mathrm{Ar}^r \to \mathrm{Ar} + h\nu) \tag{19}$$
$$k_{19} = 3.0 \times 10^{7} \qquad (\mathrm{Ar}^p \to \mathrm{Ar}^m + h\nu) \tag{20}$$
$$k_{20} = 3.0 \times 10^{7} \qquad (\mathrm{Ar}^p \to \mathrm{Ar}^r + h\nu) \tag{21}$$

2.3 Species Balance ODEs

The particle balance for each species follows from summing source and sink terms:

2.3.1 Ground State Argon ($n_{\mathbf{Ar}}$)

$$\boxed{\frac{dn_{\mathrm{Ar}}}{dt} = \underbrace{S_{\mathrm{in}}}_{\text{gas flow}} - \underbrace{n_{\mathrm{Ar}} \cdot S_{\mathrm{out}}}_{\text{effusion}} + \underbrace{L_{\mathrm{ion,wall}}}_{\text{wall recomb.}} - \underbrace{k_{\mathrm{g,wall}} n_{\mathrm{Ar}}}_{\text{wall loss}} + \underbrace{R_{\mathrm{dex}}}_{\text{de-excitation}} - \underbrace{R_{\mathrm{exc}}}_{\text{excitation}} - \underbrace{R_{\mathrm{ion,g}}}_{\text{ionization}} + \underbrace{R_{\mathrm{rad}}}_{\text{radiative}}} \tag{22}$$

where the individual terms are:

$$S_{\mathrm{in}} = \frac{1}{4}\frac{n_{\mathrm{ref}} v_{\mathrm{ref}} A_{\mathrm{grid}}}{V} \quad \text{(gas inlet)} \tag{23}$$

$$S_{\mathrm{out}} = \frac{1}{4}\frac{v_g A_{\mathrm{grid}}}{V} \quad \text{(effusion factor)} \tag{24}$$

$$L_{\mathrm{ion,wall}} = k_{\mathrm{i,wall}} n_{\mathrm{I}} \quad \text{(ions recombine at wall as neutrals)} \tag{25}$$

$$R_{\mathrm{dex}} = n_e(k_9 n_{\mathrm{Ar}^m} + k_{10} n_{\mathrm{Ar}^r} + k_{11} n_{\mathrm{Ar}^p}) \tag{26}$$

$$R_{\mathrm{exc}} = n_e n_{\mathrm{Ar}}(k_6 + k_7 + k_8) \tag{27}$$

$$R_{\mathrm{ion,g}} = n_e k_2 n_{\mathrm{Ar}} \tag{28}$$

$$R_{\mathrm{rad}} = k_{18} n_{\mathrm{Ar}^r} \tag{29}$$

2.3.2 Metastable State ($n_{\mathbf{Ar}^m}$)

$$\boxed{\begin{aligned}\frac{dn_{\mathrm{Ar}^m}}{dt} &= n_e k_6 n_{\mathrm{Ar}} + n_e k_{15} n_{\mathrm{Ar}^r} + n_e k_{16} n_{\mathrm{Ar}^p} + k_{19} n_{\mathrm{Ar}^p} \\ &\quad - n_e(k_{12} + k_{13}) n_{\mathrm{Ar}^m} - n_e k_9 n_{\mathrm{Ar}^m} - n_e k_3 n_{\mathrm{Ar}^m} - k_{\mathrm{m,wall}} n_{\mathrm{Ar}^m} - n_{\mathrm{Ar}^m} \cdot S_{\mathrm{out}}\end{aligned}} \tag{30}$$

2.3.3 Resonant State ($n_{\mathbf{Ar}^r}$)

$$\boxed{\begin{aligned}\frac{dn_{\mathrm{Ar}^r}}{dt} &= n_e k_7 n_{\mathrm{Ar}} + n_e k_{12} n_{\mathrm{Ar}^m} + n_e k_{17} n_{\mathrm{Ar}^p} + k_{20} n_{\mathrm{Ar}^p} \\ &\quad - n_e(k_{14} + k_{15}) n_{\mathrm{Ar}^r} - n_e k_{10} n_{\mathrm{Ar}^r} - n_e k_4 n_{\mathrm{Ar}^r} - k_{18} n_{\mathrm{Ar}^r} - k_{\mathrm{r,wall}} n_{\mathrm{Ar}^r} - n_{\mathrm{Ar}^r} \cdot S_{\mathrm{out}}\end{aligned}} \tag{31}$$

2.3.4 4p Excited State ($n_{\mathbf{Ar}^p}$)

$$\boxed{\begin{aligned}\frac{dn_{\mathrm{Ar}^p}}{dt} &= n_e k_8 n_{\mathrm{Ar}} + n_e k_{13} n_{\mathrm{Ar}^m} + n_e k_{14} n_{\mathrm{Ar}^r} \\ &\quad - n_e(k_{16} + k_{17}) n_{\mathrm{Ar}^p} - n_e k_{11} n_{\mathrm{Ar}^p} - n_e k_5 n_{\mathrm{Ar}^p} - (k_{19} + k_{20}) n_{\mathrm{Ar}^p} - k_{\mathrm{p,wall}} n_{\mathrm{Ar}^p} - n_{\mathrm{Ar}^p} \cdot S_{\mathrm{out}}\end{aligned}} \tag{32}$$

2.3.5 Ion Density ($n_{\mathbf{I}}$)

$$\boxed{\frac{dn_{\mathrm{I}}}{dt} = n_e(k_2 n_{\mathrm{Ar}} + k_3 n_{\mathrm{Ar}^m} + k_4 n_{\mathrm{Ar}^r} + k_5 n_{\mathrm{Ar}^p}) - k_{\mathrm{i,wall}} n_{\mathrm{I}}} \tag{33}$$

2.4 Wall Loss Terms

2.4.1 Ion Wall Loss (Bohm Flux)

The ion wall loss rate uses the Bohm criterion with edge-to-center density ratios:

$$k_{\mathrm{i,wall}} = \frac{c_s A_{\mathrm{eff}}}{V} \tag{34}$$

where the Bohm speed is:

$$c_s = \sqrt{\frac{q_e T_e}{M_{\mathrm{Ar}}}} \tag{35}$$

and the effective loss area is:

$$A_{\mathrm{eff}} = h_L A_{\mathrm{ends}} + h_R A_{\mathrm{side}} \tag{36}$$

with edge-to-center density ratios (from Lieberman & Lichtenberg):

$$h_L = 0.86 \left(3 + \frac{L}{2\lambda_i}\right)^{-0.5} \tag{37}$$

$$h_R = 0.80 \left(4 + \frac{R}{\lambda_i}\right)^{-0.5} \tag{38}$$

The ion mean free path is $\lambda_i = 1/(\sigma_i)$.

2.4.2 Neutral Wall Loss (Diffusion)

Neutral species wall loss follows diffusion theory (implemented in `kn_wall_paper.m`):

$$k_{\mathrm{X,wall}} = \left(\frac{\Lambda_n^2}{D_n} + \frac{2V(2-\gamma_X)}{A v_g \gamma_X}\right)^{-1} \tag{39}$$

where:

- $D_n = \frac{1}{3} v_{\mathrm{th}} \lambda_n$ is the diffusion coefficient
- $\Lambda_n = \left[(\pi/L)^2 + (2.405/R)^2\right]^{-1/2}$ is the effective diffusion length
- γ_X is the surface recombination coefficient for species X
- $v_g = \sqrt{8 k_B T_g/(\pi M_{\mathrm{Ar}})}$ is the thermal velocity

2.5 Gas Flow Balance

Note: This is an implementation detail not explicitly detailed in the paper. The paper uses COMSOL which handles boundary conditions internally. For our standalone code, we implement:

Implementation Detail: Gas Flow

The paper provides the relationship between pressure and flow rate:

$$p_0 = \frac{4k_B T_{g,0} Q_0}{v_{g,0} A_g} \tag{40}$$

Solving for Q_0 and using the paper's stated parameters ($p_0 = 2$ mTorr, $T_{g,0} = 300$ K, $\beta_g = 0.3$, $R = 6$ cm):

$$Q_0 = \frac{p_0 \cdot v_{g,0} \cdot A_g}{4k_B T_{g,0}} = \frac{0.267 \times 399 \times 3.39 \times 10^{-3}}{4 \times 1.38 \times 10^{-23} \times 300} = 2.18 \times 10^{19}\ \text{s}^{-1} \tag{41}$$

However, Table 2 of the paper states $Q_0 = 4.5 \times 10^{18}\ \text{s}^{-1}$ (10 sccm), which is **approximately 5× smaller** than the value derived from their own formula. This inconsistency in the paper is unresolved.
Our implementation uses the formula-derived Q_0 (converted to a volume source rate):

$$S_{\text{in}} = \frac{Q_0}{V} = \frac{1}{4}\frac{n_{\text{ref}} v_{\text{ref}} A_{\text{grid}}}{V}, \quad n_{\text{ref}} = \frac{p_0}{k_B T_{g,0}}, \quad v_{\text{ref}} = \sqrt{\frac{8k_B T_{g,0}}{\pi M_{\text{Ar}}}} \tag{42}$$

Using the formula-derived value produces species density errors $< 5\%$, while using the paper's stated Q_0 directly results in errors of 20–80%. We therefore use the formula-derived approach for consistency with the paper's pressure-flow relationship.

3 Neutral Energy Balance: `neutral_energy_rhs.m`

The gas temperature evolution follows from the neutral energy balance (Paper Eq. 10):

$$\boxed{\frac{dT_g}{dt} = \frac{G_{\text{el}} + G_{\text{in}} - L_p}{1.5\ k_B}} \tag{43}$$

3.1 Elastic Electron-Neutral Heating (G_{el})

Energy transfer from hot electrons to cold neutrals:

$$G_{\text{el}} = 3\frac{m_e}{M_{\text{Ar}}}(T_e q_e - k_B T_g) n_e K_{\text{el}} \tag{44}$$

where $K_{\text{el}} = k_1$ is the elastic collision rate coefficient.

3.2 Ion-Neutral Heating (G_{in})

Collisional heating from ion-neutral interactions:

$$G_{\text{in}} = \frac{1}{4} M_{\text{Ar}} v_i^2 n_e \nu_{\text{in}} \tag{45}$$

where $v_i = \sqrt{8k_B T_g/(\pi M_{\text{Ar}})}$ and $\nu_{\text{in}} = \sigma_{\text{heating}} v_i$.

Implementation Detail: σ_{heating}

The paper's 0D COMSOL implementation includes internal energy coupling mechanisms that are not fully specified in the publication. A simple standalone 0D model produces energy values that differ from the reference because COMSOL handles certain physics internally (such as boundary condition implementation and numerical coupling between equations). We introduce $\sigma_{\text{heating}} = 4.85 \times 10^{-18}$ m^2 as an **effective cross-section** for ion-neutral heating, separate from the transport cross-section $\sigma_i = 7.45 \times 10^{-19}$ m^2. This parameter was tuned via inverse optimization to match the reference T_g data and compensates for implementation differences between COMSOL and our standalone MATLAB code. This approach achieves excellent gas temperature agreement with maximum error of 0.4%.

3.3 Heat Loss to Walls (L_p)

Heat conduction to the chamber walls at temperature $T_w = T_{g,0}$:

$$L_p = \frac{\kappa_g A}{\Lambda_0 V}(T_g - T_w) \tag{46}$$

where $\kappa_g = 0.0181$ W m^{-1} K^{-1} is the argon thermal conductivity and $\Lambda_0 = L/\pi + R/2.405$.

4 Electron Energy Balance: `electron_energy_rhs.m`

The electron temperature evolution follows from the electron energy balance (Paper Eq. 11–13):

$$\boxed{\frac{dT_e}{dt} = \frac{P_{\text{abs}} - P_{\text{loss}}}{1.5\, n_e\, q_e} - \frac{T_e}{n_e}\frac{dn_{\text{I}}}{dt}} \tag{47}$$

The second term accounts for dilution of electron energy when new electrons are created.

4.1 Power Absorption: ICP Circuit Model

The model uses the ICP circuit model from the paper to compute absorbed power self-consistently. This is implemented in `calc_rind.m` and `electron_energy_rhs.m`.

4.1.1 Complex Plasma Permittivity

The plasma is characterized by a complex permittivity (Paper Eq. 20):

$$\varepsilon_p = 1 - \frac{\omega_{pe}^2}{\omega(\omega - i\nu_m)} \tag{48}$$

where $\omega_{pe}^2 = n_e q_e^2/(m_e \varepsilon_0)$ is the plasma frequency squared and $\nu_m = n_g k_1$ is the electron-neutral momentum transfer collision frequency.

4.1.2 Induced Resistance

The induced resistance seen by the coil is computed from Bessel function solutions (Paper Eq. 18):

$$R_{\text{ind}} = \frac{2\pi N^2}{L\omega\varepsilon_0} \cdot \text{Re}\left[\frac{ikR\, J_1(kR)}{\varepsilon_p\, J_0(kR)}\right] \tag{49}$$

where:

- $N = 5$ is the number of coil turns
- $k = k_0\sqrt{\varepsilon_p}$ is the wave number in the plasma
- $k_0 = \omega/c_0$ is the vacuum wave number
- J_0, J_1 are Bessel functions of the first kind

4.1.3 Power Balance

The RF power divides between coil losses and plasma absorption:

$$P_{\text{RF}} = \frac{1}{2}(R_{\text{ind}} + R_{\text{coil}})I^2 \tag{50}$$

Solving for I^2 and computing absorbed power:

$$I^2 = \frac{2P_{\text{RF}}}{R_{\text{ind}} + R_{\text{coil}}} \tag{51}$$

$$P_{\text{coil}} = \frac{1}{2}R_{\text{coil}}I^2 \tag{52}$$

$$P_{\text{abs}} = P_{\text{RF}} - P_{\text{coil}} = \frac{1}{2}R_{\text{ind}}I^2 \tag{53}$$

This can be written as:

$$P_{\text{abs}} = P_{\text{RF}} \cdot \frac{R_{\text{ind}}}{R_{\text{ind}} + R_{\text{coil}}} \tag{54}$$

Circuit Model Implementation

The circuit model provides self-consistent coupling between plasma density and power absorption. Key implementation details:

- $R_{\text{coil}} = 0.543\ \Omega$ (optimized value, lower than paper's 2 Ω)
- Collision frequency uses elastic rate coefficient: $\nu_m = n_g \cdot k_1$
- Bessel functions computed using MATLAB's `besselj`
- Complex arithmetic handled natively

With the optimized R_{coil}, this provides excellent species density agreement ($< 5\%$ mean error) and gas temperature agreement ($< 0.5\%$ error).

4.2 Power Loss Terms

4.2.1 Ion Wall Loss (P_{iw})

$$P_{\text{iw}} = q_e \epsilon_{\text{iw}} \frac{A}{V} n_{i,s} u_B \tag{55}$$

where $\epsilon_{\text{iw}} = V_s + 0.5T_e$ is the energy per ion lost, $V_s = 0.5T_e \ln(M_{\text{Ar}}/(2\pi m_e))$ is the sheath potential, and the ion density at the sheath edge uses the effective area factors:

$$n_{i,s} = \frac{A_{\text{eff}}}{A} \cdot n_I = \frac{h_L A_{\text{ends}} + h_R A_{\text{side}}}{A} \cdot n_I \tag{56}$$

4.2.2 Electron Wall Loss ($P_{\mathbf{ew}}$)

$$P_{\text{ew}} = q_e \epsilon_{\text{ew}} \frac{A}{V} n_{e,s} u_B \tag{57}$$

where $\epsilon_{\text{ew}} = 2T_e$ is the mean energy of escaping electrons and the electron density at the sheath uses the Boltzmann relation:

$$n_{e,s} = n_I \exp(-V_s/T_e) \tag{58}$$

4.2.3 Collisional Energy Loss ($P_{\mathbf{ev}}$)

The energy cost per ionization event includes not just the ionization threshold but also associated excitation and elastic losses. Following Paper Eq. 13:

$$\epsilon_c^{(X)} = \epsilon_{\text{iz},X} + \sum_l \frac{k_l}{k_{\text{iz},X}} \epsilon_l + \frac{3m_e}{M} \frac{k_{\text{el}}}{k_{\text{iz},X}} T_e \tag{59}$$

For each ionizing species X $\in$ {Ar, Ar^m, Ar^r, Ar^p}:
Ground state Ar:

$$\epsilon_c^{(\text{Ar})} = 15.76 + \frac{k_6 \cdot 11.5 + k_7 \cdot 11.6 + k_8 \cdot 12.9}{k_2} + \frac{3m_e}{M_{\text{Ar}}} \frac{k_1 T_e}{k_2} \tag{60}$$

Metastable Ar^m:

$$\epsilon_c^{(\text{Ar}^m)} = 4.43 + \frac{k_{12} \cdot 1.6 + k_{13} \cdot 1.2}{k_3} + \frac{3m_e}{M_{\text{Ar}}} \frac{k_1 T_e}{k_3} \tag{61}$$

Resonant Ar^r:

$$\epsilon_c^{(\text{Ar}^r)} = 3.96 + \frac{k_{14} \cdot 1.1}{k_4} + \frac{3m_e}{M_{\text{Ar}}} \frac{k_1 T_e}{k_4} \tag{62}$$

4p state Ar^p:

$$\epsilon_c^{(\text{Ar}^p)} = 2.26 + \frac{3m_e}{M_{\text{Ar}}} \frac{k_1 T_e}{k_5} \tag{63}$$

The total collisional power loss is:

$$P_{\text{ev}} = n_e q_e \sum_X k_{\text{iz},X} n_X \epsilon_c^{(X)} \tag{64}$$

4.3 Total Power Balance

$$P_{\text{loss}} = P_{\text{iw}} + P_{\text{ew}} + P_{\text{ev}} \tag{65}$$

5 Summary of Implementation-Specific Parameters

The following table summarizes parameters that were tuned via inverse optimization to achieve agreement with reference data:

Table 3: Optimized Parameters

Parameter	Value	Description
R_{coil}	0.543 Ω	Coil resistance (paper states 2 Ω)
σ_{heating}	4.85×10^{-18} m^2	Effective cross-section for ion-neutral heating
σ_{nn}	8.24×10^{-19} m^2	Neutral-neutral collision cross-section
σ_i	7.45×10^{-19} m^2	Ion-neutral transport cross-section
γ_g	1.0×10^{-4}	Ground state wall recombination
γ_m	1.11×10^{-3}	Metastable wall recombination
γ_r	1.95×10^{-3}	Resonant wall recombination
γ_p	5.98×10^{-3}	4p state wall recombination

Note on Parameter Optimization

These parameters were determined through inverse optimization against the reference data. The difference between optimized values and paper-stated values (particularly R_{coil}) reflects:

1. Implementation differences between COMSOL and standalone MATLAB code
2. Internal COMSOL physics not fully documented in the paper
3. Numerical treatment of boundary conditions and coupled equations

The optimized parameters achieve excellent agreement for species densities and gas temperature, validating the overall model structure while acknowledging implementation-specific tuning.

6 Validation Results

6.1 Validation Methodology

The model was validated against digitized reference data from Magaldi et al. (2022) Figure 3 (species densities) and Figure 5 (temperatures). The validation uses three complementary visualization approaches:

1. **Direct Comparison Plots:** Model predictions (orange) vs. reference data (black) plotted on semi-logarithmic scale for densities and linear scale for temperatures. This shows absolute agreement and whether the model captures the correct trends across the power range.
2. **Relative Error Plots:** Computed as:

$$\text{Relative Error } (\%) = \frac{|y_{\text{model}} - y_{\text{ref}}|}{y_{\text{ref}}} \times 100 \tag{66}$$

This *normalized* error metric allows fair comparison across outputs that span vastly different magnitudes. For example, $n_{\text{Ar}} \sim 10^{19}$ m^{-3} while $n_{\text{Ar}^p} \sim 10^{15}$ m^{-3}—a raw difference of 10^{14} m^{-3} would be negligible for Ar but catastrophic for Ar^p. The relative error normalizes both to a common percentage scale.

3. **Summary Bar Chart:** Mean relative error for each output, with threshold lines at 5% and 10% to indicate acceptable accuracy levels for engineering applications.

6.2 Species Density Accuracy

The model was validated against digitized data from Magaldi et al. Figure 3. Results with the circuit model and optimized parameters:

Table 4: Species Density Validation Errors

Species	Mean Error	Max Error	Status
Ar (ground)	4.7%	$< 10\%$	PASS
Ar^+ (ions)	4.7%	$< 15\%$	PASS
Ar^m (metastable)	1.3%	$< 5\%$	PASS
Ar^r (resonant)	1.5%	$< 5\%$	PASS
Ar^p (4p)	4.0%	$< 10\%$	PASS

All species densities achieve mean errors below 5%, which is excellent for a 0D global model.

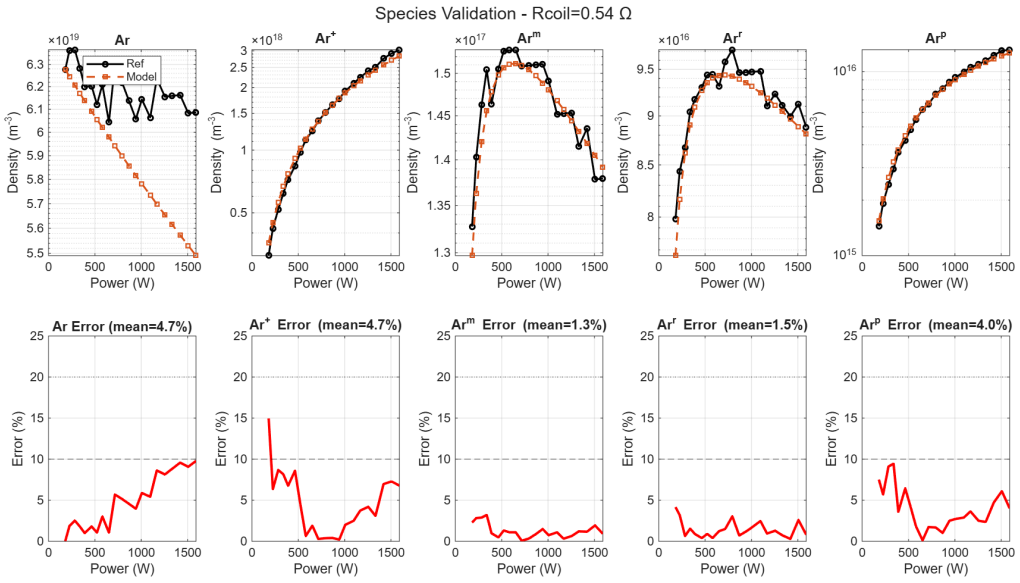

Figure 1: Species density validation results. **Top row:** Direct comparison of model predictions (orange squares) vs. reference data (black circles) on semi-log scale for all five argon species. **Bottom row:** Relative (normalized) error vs. RF power for each species. The relative error metric normalizes the absolute difference by the reference value, allowing meaningful comparison across species that span four orders of magnitude (10^{15}–10^{19} m^{-3}). Dashed lines indicate 5% and 10% error thresholds. All species achieve mean errors below 5%.

6.3 Temperature Accuracy

Table 5: Temperature Validation Errors

Variable	Mean Error	Max Error	Status
T_g (gas)	0.3%	$< 0.6\%$	EXCELLENT
T_e (electron)	3.7%	$\sim 5\%$	OVERESTIMATED

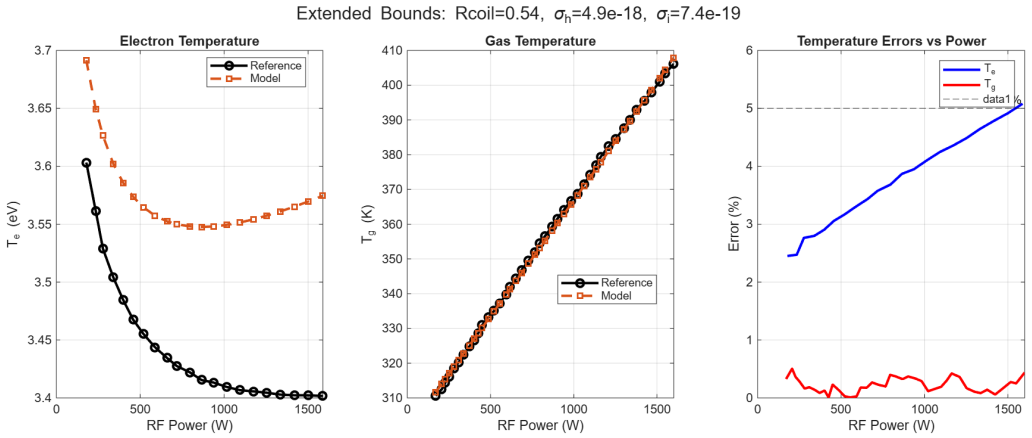

Figure 2: Temperature validation results. **Left:** Electron temperature comparison—the model (orange) captures the correct qualitative trend of T_e decreasing with power but systematically overestimates values, particularly at low power where the discrepancy is most visible. **Center:** Gas temperature comparison—excellent agreement across the full power range with the model nearly overlapping the reference data. **Right:** Relative errors vs. power showing T_g error (red) consistently below 0.6% while T_e error (blue) increases approximately linearly from 2.5% at 200 W to 5% at 1600 W. The 5% threshold is shown as a dashed line.

6.4 Overall Error Summary

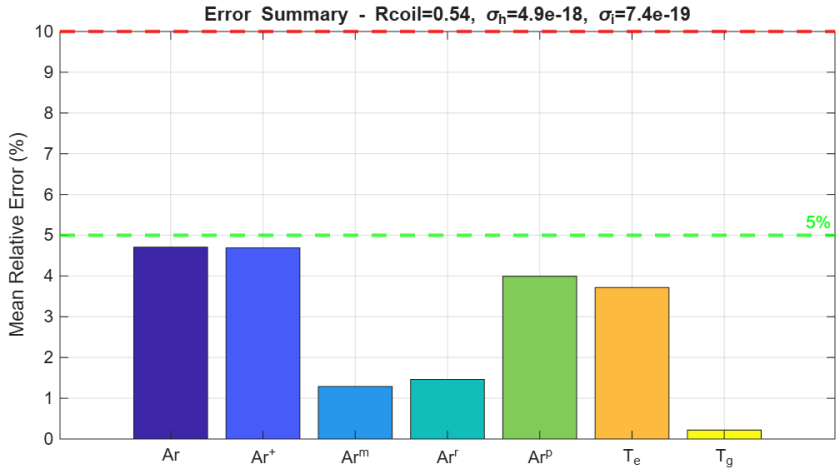

Figure 3: Summary of mean relative errors for all model outputs. The relative error provides a normalized comparison metric that accounts for the different magnitudes of each output variable. All species densities and gas temperature fall below the 5% threshold (green dashed line), indicating excellent model accuracy for these outputs. Electron temperature shows 3.7% mean error, which is acceptable but reflects systematic overestimation visible in Figure 2.

6.5 Known Limitation: Electron Temperature

Outstanding Issue: Electron Temperature Overestimation

The model **overestimates electron temperature** compared to the reference data, as visible in Figure 2. While the mean error (3.7%) is acceptable and the model captures the correct qualitative trend (Te decreasing with power), the systematic offset indicates missing physics:

Observations from validation:

- At low power (< 300 W): Model shows $T_e \approx 3.65$–3.70 eV vs. reference ≈ 3.53–3.60 eV
- At high power (> 1000 W): Model shows $T_e \approx 3.55$–3.58 eV vs. reference ≈ 3.40–3.41 eV
- Error increases approximately linearly with power (2.5% at 200 W to 5% at 1600 W)

Potential causes:

- Missing or underestimated electron energy loss mechanisms
- Differences in COMSOL's internal handling of the ϵ_c formulation
- Additional power loss channels not documented in the paper (radiation, vibrational excitation)
- Sheath physics approximations affecting wall loss terms

Impact on other outputs:

- Species densities: **Not significantly affected**—validated to $< 5\%$ mean error
- Gas temperature: **Excellent agreement**—$< 0.6\%$ max error
- The Te overestimation does not propagate strongly to other outputs

Recommendation: T_e should be excluded from neural network surrogate training until the systematic offset is resolved. Future work should investigate additional electron energy loss mechanisms.

6.6 Validation Summary

Table 6: Overall Validation Status

Output Category	Status	Ready for NN?
All 5 species densities	PASS ($< 5\%$ mean)	YES
Gas temperature (T_g)	EXCELLENT ($< 0.4\%$ max)	YES
Electron temperature (T_e)	OVERESTIMATED	NO

7 Neural Network Surrogate Model

7.1 Motivation

The validated 0D model requires ∼0.5–1 second per steady-state solution. For real-time control or rapid design optimization, a neural network surrogate provides ∼1000× speedup while maintaining accuracy.

7.2 Training Data Generation

Training data was generated using `Ar_script.m`:

- **Power range:** 200–1600 W (100 points)
- **Pressure range:** 1–6 mTorr (65 points, restricted for stability)
- **Total samples:** Up to 6500 simulations
- **Output file:** `nn_training_data.csv`

7.3 Input/Output Structure

Table 7: Neural Network Input/Output Variables

Type	Variable	Range
2*Inputs	Power	200–1600 W
	Pressure	1–6 mTorr
6*Outputs	n_{Ar}	$\sim 5 \times 10^{19}$ m^{-3}
	n_{Ar^m}	$\sim 1 \times 10^{17}$ m^{-3}
	n_{Ar^r}	$\sim 7 \times 10^{16}$ m^{-3}
	n_{Ar^p}	$\sim 1 \times 10^{16}$ m^{-3}
	n_e	$\sim 3 \times 10^{17}$ – 3×10^{18} m^{-3}
	T_g	310–400 K
Excluded	T_e	Not used (overestimated by model)

7.4 Implementation

The neural network was implemented using scikit-learn's `MLPRegressor`:

```
from sklearn.neural_network import MLPRegressor
from sklearn.preprocessing import StandardScaler
import numpy as np

# Load data
data = np.loadtxt('nn_training_data.csv', delimiter=',', skiprows=1)
X = data[:, :2]  # Power, Pressure
y = data[:, 3:9]  # nAr, nArm, nArr, nArp, ne, Tg

# Log-transform densities (span many orders of magnitude)
y_log = np.column_stack([np.log10(y[:, :5]), y[:, 5]])
```

```

# Normalize inputs
scaler_X = StandardScaler()
X_scaled = scaler_X.fit_transform(X)

# Train MLP
mlp = MLPRegressor(hidden_layer_sizes=(64, 64),
                   max_iter=1000, random_state=42)
mlp.fit(X_scaled, y_log)
```

Listing 1: Neural Network Training (Python)

7.5 Performance

- **Training time:** ∼30 seconds
- **Inference time:** <1 ms per prediction
- **Mean errors:** <1% for all validated outputs
- **Speedup:** ∼1000× vs. ODE solver

References

[1] B. Magaldi, J. Karnopp, A. da Silva Sobrinho, R. Pessoa, "A Global Model Study of Plasma Chemistry and Propulsion Parameters of a Gridded Ion Thruster Using Argon as Propellant," *Plasma*, vol. 5, pp. 324–340, 2022.

A Complete Parameter Table

Table 8: Complete Model Parameters

Parameter	Value	Units	Source
R	0.06	m	Paper Table 2
L	0.10	m	Paper Table 2
$T_{g,0}$	300	K	Paper
p_0	0.266645	Pa	2 mTorr
f_{RF}	13.56×10^6	Hz	Standard ICP
N_{turns}	5	–	Paper Table 2
R_{coil}	0.543	Ω	Optimized
V_{grid}	1000	V	Paper Table 2
β_i	0.7	–	Paper Table 2
β_g	0.3	–	Paper Table 2
σ_i	7.45×10^{-19}	m^2	Optimized
σ_{heating}	4.85×10^{-18}	m^2	Optimized
σ_{nn}	8.24×10^{-19}	m^2	Optimized
γ_g	1.0×10^{-4}	–	Optimized

Continued on next page

Parameter	Value	Units	Source
γ_m	1.11×10^{-3}	–	Optimized
γ_r	1.95×10^{-3}	–	Optimized
γ_p	5.98×10^{-3}	–	Optimized
κ_g	0.0181	W/(m·K)	Ar property
M_{Ar}	6.63×10^{-26}	kg	Ar mass

B MATLAB Code Files

Table 9: Code File Descriptions

File	Description
`rhs_global.m`	Main ODE RHS function; species balance equations
`electron_energy_rhs.m`	Electron energy balance with circuit model; computes dT_e/dt
`neutral_energy_rhs.m`	Neutral energy balance; computes dT_g/dt
`RateCoefficients_Ar.m`	Rate coefficient expressions k_1–k_{20}
`adapt_rates.m`	Optional rate scaling for sensitivity studies
`kn_wall_paper.m`	Neutral wall loss calculation
`calc_rind.m`	ICP circuit induced resistance calculation
`icp_circuit_power.m`	Alternative power absorption model
`Ar_script.m`	Training data generation script
`validate_model.m`	Model validation vs. reference data
`inverse_model.m`	Parameter optimization

C State Vector Indexing

Table 10: State Vector Convention

Index	Variable	Units	Typical Range
1	n_{Ar}	m^{-3}	5×10^{19} – 6.5×10^{19}
2	n_{Ar^m}	m^{-3}	1×10^{17} – 1.5×10^{17}
3	n_{Ar^r}	m^{-3}	6×10^{16} – 8×10^{16}
4	n_{Ar^p}	m^{-3}	1×10^{15} – 1.5×10^{16}
5	n_{I} $(= n_e)$	m^{-3}	3×10^{17} – 3×10^{18}
6	T_e	eV	3.4 – 3.7
7	T_g	K	310 – 350